Chapter 2
Drought Variability and Land Degradation in Central Asia: Assessment Using Remote Sensing Data and Drought Indices

Dildora Aralova, Jahan Kariyeva, Timur Khujanazarov, and Kristina Toderich

Abstract The regional resilience of a landscape to climate change in water-scarce areas is one of the core environmental problems nowadays for Central Asian countries. Responses to increasing temperature and high evapotranspiration (ET_0) regimes have contributed to biodiversity loss and altered vegetation dynamics and changed the land use and management in these landscapes. Extremely dry conditions and droughts are recognized as an important factor that triggers land degradation in Central Asia. The aim of this study is to conduct attribution analysis to assess drought trends that are quantified using the Standardized Precipitation-Evapotranspiration Index (SPEI) and effects of other biophysical factors on the region and at a country level. The kriging (geostatistics) method was utilized to predict the status of vegetation change trends and generalize additive smoothed parameters to provide response factors for changes of land cover status. Specific

D. Aralova (✉)
Dresden Technology University (TU-Dresden), Institute of Photogrammetry and Remote Sensing, Dresden, Germany

Centre of Hydrometeorological Service at Ministry of Emergency Situations of the Republic of Uzbekistan (Uzhydromet), Tashkent, Uzbekistan
e-mail: aralovad@daad-alumni.de

J. Kariyeva
Alberta Biodiversity Monitoring Institute, Edmonton, AB, Canada
e-mail: kariyeva@ualberta.ca

T. Khujanazarov
Water Resources Research Center, Disaster Prevention Research Institute, Kyoto University, Uji, Japan

K. Toderich
ICBA-CAC (International Center for Bio-saline Agriculture in Central Asia and Caucasus), ICARDA Regional Office (The CGIAR Facilitation Unit) for CAC, Tashkent, Uzbekistan
e-mail: ktoderich@cgiar.org

D. Egamberdieva, M. Öztürk (eds.), *Vegetation of Central Asia and Environs*,
https://doi.org/10.1007/978-3-319-99728-5_2

objectives of the study were (a) *to assess drought trends and their effects on climate–vegetation trends at the regional and local level*; (b) *identify the main affected regions among five countries* (Kazakhstan, Kyrgyzstan, Tajikistan, Turkmenistan, and Uzbekistan) and *characterize their patterns for monitoring land tenures*; and (c) *define appropriate ecological risk zones*, especially trends of spatial changes over time with drought trends. The simulated and predicted maps with kriging dependence terms indicated that the climate–vegetation-driven dataset will suffer substantial losses of vegetation health [normalized difference vegetation index (NDVI)] in precipitation-driven regions of Turkmenistan, Uzbekistan, and Tajikistan, and that these areas, especially, Ahal and Lebap Provinces in Turkmenistan, Kyzylorda in Kazakhstan, Karakalpakstan Autonomous Republic in Uzbekistan, and Gorno-Badakhsan Autonomous Region (GBAR) in Tajikistan, are very sensitive to droughts, which might alert us to the fragility of this ecosystem.

Keywords Central Asia · Droughts · SPEI · NDVI-GIMMS3g · Precipitation · CRU-TS, kriging method

2.1 Introduction

Approximately 75% of the land in Central Asia (Kazakhstan, Kyrgyzstan, Tajikistan, Turkmenistan, and Uzbekistan) is occupied by rangelands (Bedunah et al. 2006); the total area of pastures in Central Asia is 262 million hectares (ha) (Squires 2012). Sustainable management of rangelands is a key goal for Central Asian countries, and the main challenge today is to conserve and restore ecosystems that are vital to human well-being. The effects of shrinking the Aral Sea Basin (Toderich et al. 2013) coupled with the USSR (Soviet Union) collapse have caused changes in land use practices (Kariyeva 2011), such as uncontrolled grazing, which lead to salinization and further deterioration of rangeland ecosystems (Aralova et al. 2016) in the region. During the USSR period, most of the agricultural policies were directed by the centralized government's decisions, which contributed strongly to degradation of dryland areas. A longer drought events and subsequent soil salinization are threats that have major impacts on land cover and land use change (LCLUC) patterns in the agricultural zones of Central Asia. The anthropogenic impact of converting vast dryland areas to irrigated lands, coupled with the accelerated increase of average temperature (as drivers) and precipitation anomalies observed in past decades, has been changing LCLUC dynamics in those areas. According to Nicholson et al. (1998) and Pickup (1998), drought has been considered to be a major factor in triggering land degradation and increasing desertification categories. However, some studies have argued that drought cannot be a factor explaining degradation trends (Vicente-Serrano et al. 2015a, b).

Central Asian countries still attribute 10–25% of their gross domestic product (GDP) to agriculture (FAOstat 2015). Large areas of steppe rangelands are used as pastures for breeding cattle, where it is the main income source for the rural popula-

tion; also, 20–50% of the total employment rate is acquired in the agricultural sector (FAOstat 2015). Agriculture remains is an important sector in the economy of Central Asia, contributing 5.2% of the GDP in Kazakhstan, 7.5% in Turkmenistan, 18.5% in Uzbekistan, 20.8% in Kyrgyzstan, and 23.3% in Tajikistan (Abdullaev 2014; Bobojonov and Aw-Hassan 2014). The financial capacity of most countries is not robust enough to allocate adequate funds for drought management and mitigation, or for large-scale relief operations in the agriculture sector, especially in the developing or least developed countries. However, a number of remote sensing–based vegetation and drought indices have been developed for use in estimating vegetation status (such as the normalized difference vegetation index, NDVI) and degradation level, and Vegetation Drought Response Index (VegDRI) studies have begun to investigate the use for a drought-monitoring system in the United States (Wardlow et al. 2012a, b). The VegDRI targets the effects of drought on vegetation with applying general vegetation conditions (soil, elevation, etc.) and ratings of dryness extended by applying climate-based drought indices. Different algorithms have been proposed in drought research (Paulik et al. 2014; Ciabatta et al. 2016; Musyimi 2011; Kerr et al. 2012), but these are generally based on the exploitation of the available datasets (satellite derived), and suitable implementation for Central Asian landscapes has not yet been done. Severe to extreme drought conditions are causing a serious issue in dryland ecosystems, and the effects of drought on vegetation patterns in Central Asia were evident several times in the past two decades, and observations in various regions (Kariyeva and van Leuwen 2010) also affirmed these assumptions. In drylands, during a period with a high-temperature trend (June–August), drought days will increase more than three times in most areas of Central Asia at the end of the twenty-first century (Touge et al. 2015). Therefore, contradictory extremes (high rainfall ratings and hot temperature) are also negative influences on this landscape. As mentioned, there are still large gaps in managing or forecasting with contributing/creating an early warning system in the region level. In Central Asia, approximately 80% of rural people are involved in the agricultural sector, and the landscape of this area is vulnerable to droughts. As well, as can be drawn from the episode years of 2000–2001, such droughts hit in all five countries, resulting in rainfall levels decreasing below average (approximately 60% to 40%); and river flows dropping by 35–40% from those in a normal period. According to the accounts of Mirzabaev et al. (2015), the cost of land degradation categorized between 2001 and 2009 in Central Asia was estimated to be about $6 billion annually, as the result of rangeland degradation ($4.6 billion), followed by desertification ($0.8 billion), deforestation ($0.3 billion), and abandonment of croplands ($0.1 billion). As a result, most regions of the area were unable to manage disaster risks and to effectively recover from disasters.

A few analyses and studies provide for accurately quantifying drought trends and anomalies and finding relationships with vegetation pattern dynamics for these landscapes. Many researchers have analyzed vegetation sensitivity to climate trends (Propastin et al. 2008; Kariyeva 2011) between precipitation episodes (Gessner et al. 2012).

Drought indices such as the Standardized Precipitation Evapotranspiration Index (SPEI) allows drought severity to be compared through time and space, as it has estimated over a wide range of climates. A different scientific discipline enables detection, monitoring, and analysis of droughts and drought indices (Vicente-Serrano et al. 2015a, b). In this chapter, various satellite-based datasets were used and evaluated under kriging methodology, with the aim to forecast upcoming warming regions or sensitive areas in upcoming drought years or vegetation health threats in the case of Central Asia. As examples, we selected Lebap (Turkmenistan), Navoi (Uzbekistan), Kyzylorda (Kazakhstan), the Gorno-Badakhshan Autonomous Region (GBAR; Tajikistan), Ulytau (Kazakhstan), and Naryn (Kyrgyzstan).

The SPEI was calculated with the Penman–Monteith method following the work of Vicente-Serrano et al. (2017) and linking-based practices for drought risk reduction. The kriging method might be able to evaluate and understand the strength of NDVI drought–climate relationships and further reducing or warning of disaster risks in Central Asia. Rangeland diversity in Central Asia remains one of the important tasks of the Central Asian countries, understanding past and current conditions (Gintzburger et al. 2003) and forecasting future status. Also, it is important to provide measures for delay periods as reported by Udelhoven et al. (2009) and Gasparrini (2011), and to establish an adaptation mechanism for arid ecosystems. Especially between boundary countries and remote areas, adaptation strategies with action plans must be evaluated in various biodiversity loss areas of Central Asia.

2.2 Materials and Methods

2.2.1 Location

Central Asia includes a range of landscapes from mountains to steppes and deserts (Turkmenistan, Kazakhstan, and Uzbekistan) and is isolated by mountain ranges (Kyrgyzstan, Tajikistan) and the Caspian Sea (the borders with Turkmenistan, partly with Kazakhstan). The spatial extent of dryland rangelands in Central Asia is vast. The vegetation trends in this area (Fig. 2.1a) are mostly driven by precipitation and temperature dynamics; for example, warming temperature trends after spring lead to increasing NDVI values. As evaluated, non-cropland area is dominated by rangelands and mostly used in the agricultural sector for short-term crop rotation (Fig. 2.1b). As described on the mapped part of Central Asia (Fig. 2.2), the annual ascending ratings of precipitation are highly distributed mostly throughout the mountainous zones of Central Asia (Tajikistan and part of Kyrgyzstan), and more precipitation occurs on the eastern side of the regions than on the other sides of Central Asia.

In general, the objectives of this research are to assess and identify possible decreasing vegetation trends with quantifying SPIE trends and may enable under-

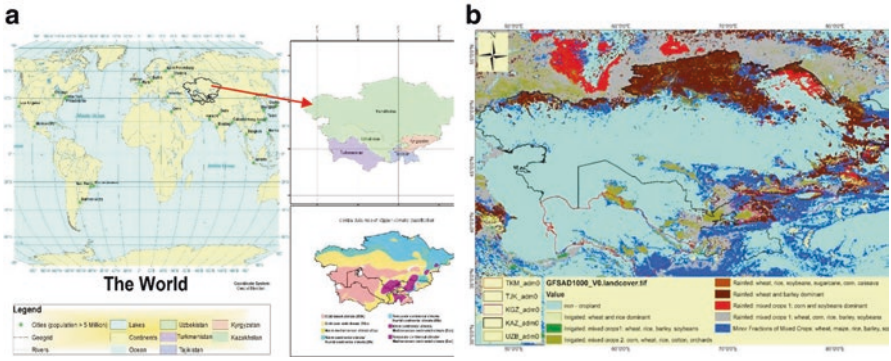

Fig. 2.1 Target area description: location of the middle zone of Asian continent (left) and climate classifications based on assumptions of Koeppen methodology (right). (**a**) Location of Central Asia and five neighbor countries and functional relationships with potential climate attributes in regions. Reference system: WGS84. Central Asian map with Köppen climate classification (right, down) with extraction permanent water attributes. (**b**) Central Asian Cropland Extent and Crop Dominance, modified after GFSAD1000 V0.0 Classes. Image resolution is aggregated to 500 m and projected to the Central Eurasian part from global cropland extent project. Accessed Google Earth Engine, May 2017 (Thenkabail et al. 2012)

standing the mechanism of land degradation in Central Asia or the regional scale of degradation within implementing various drivers, for example, Köppen classification, land use dynamics, and land cover dynamics.

2.2.1.1 Climatic Parameters and Description.

Precipitation in Central Asia Between 1982 and 2015

The analysis of spatial resolution observed by Gong et al. (2017) mentioned that high-value centers of precipitation appear in Kyrgyzstan, and then in Tajikistan. Our findings show similarity, the only exceptions being Turkmenistan, in that Turkmenistan has high precipitation accumulation ratings only for the eastern side. Accumulated high–moderate rating areas are the western part of Uzbekistan, the northern and northwestern part of Kazakhstan, and the northern part of Turkmenistan. Generally, the Central Asia precipitation trend has increased in some regions, especially in the month of May, 2015, in Kazakhstan; the opposite contradictions happened also in the southern areas such as Uzbekistan (eastern side) and Turkmenistan (northeastern side), where the precipitation trends were decreased from November months until February (trends are seen in Fig. 2.2). Accounting yearly values of precipitation also described that in that part of Kazakhstan, Kyrgyzstan and Uzbekistan have raised precipitation ratings for the year 2015. Even a peak of precipitation trends was seen in Kazakhstan in 2015, which was troubled with waterlogging in the north, and on the northwestern side of

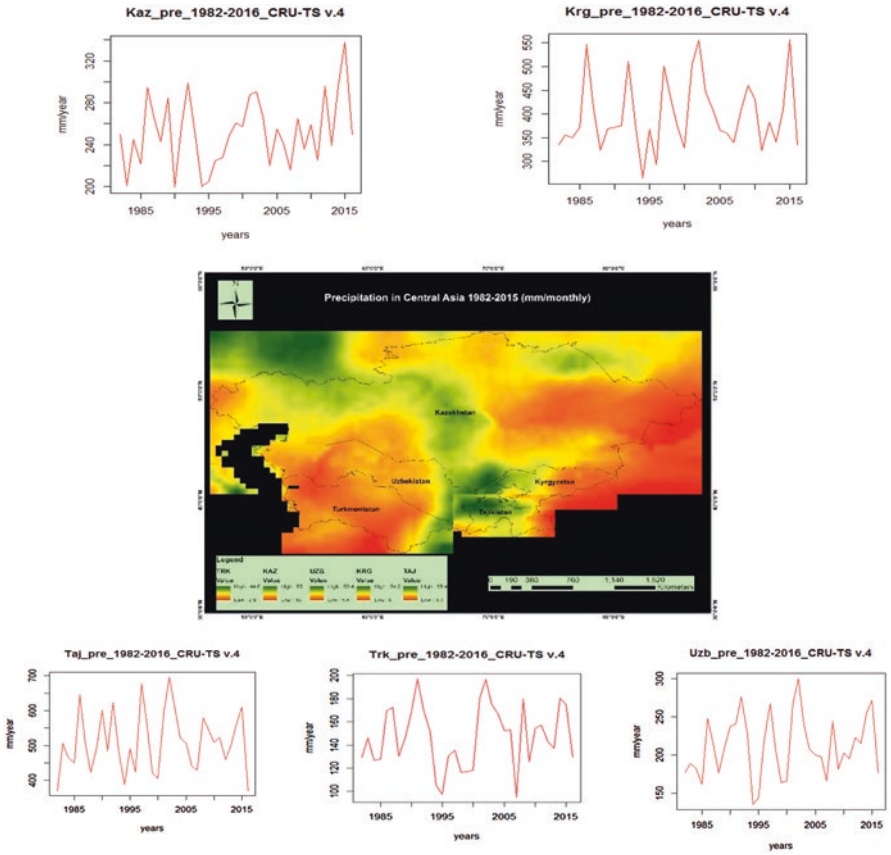

Fig. 2.2 Precipitation trends in the five countries estimated from the period 1982–2015 and illustrated yearly contributions (up side and down side) and monthly mapping of precipitation (in the middle) in Central Asia for the same period. All datasets based on CRU-TS 4 version

Kazakhstan. At the same time, the rate of ET_0 is increased (not shown) and continued at least 90 days per year in these regions. In those periods, land surface precipitation reached 0–10 mm/month. Results show that under climatic conditions in which low annual variability of precipitation predominates (Turkmenistan, Uzbekistan, part of Kazakhstan), the drought indices respond mainly as higher negative trends. Also, annually trends of precipitation is responding on high productivity of the rainfed zones, and these areas are generally for Kazakhstan, Tajikistan, and Kyrgyzstan, where drought indices contributing positively on mostly estimated periods and as well as, some years also contributed as negative. These selected and targeted areas are dependent on rainfall rates. But, controversy also occurs. At the same time, in these areas the hottest period of summer was

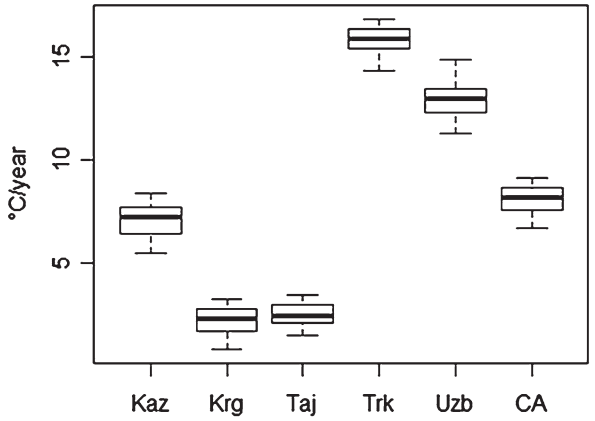

Fig. 2.3 Boxplot of annual average temperature in Central Asian countries based on monthly dataset CRU-TS ver.4 and generally for Central Asia

observed, after heavy rainfall (in 2015). However, the temperature ratings estimations are based on annual average calculations (Fig. 2.3), and, in fact, the sum of annual rainfall was greater than <500 mm/yearly; the environment or temperature is cooler in this country, similar to Tajikistan and Kyrgyzstan (Fig. 2.2).

2.2.2 Classification of Targeted Area

As shown on Fig. 2.1a, three main categories apply in the south and southwestern parts of Central Asia (Table 2.1): the categories with letter "*B*" are classified as *desert zones* and the main criteria for this category are MAP $<5 \times P^{1}_{\text{threshold}}$; obviously the Köppen categories are described as a high ET_0 and zones of less precipitation (Fig. 2.1a) and occupy the south and southwestern parts (Turkmenistan, Uzbekistan, and in part the southwestern side of Kazakhstan) of Central Asia (see Fig. 2.1b). The "BWk" category is mostly contributed in Central Asia. Multidisciplinary analysis of climatic drivers that are modified by the Köppen classification provides a visual interpretation of vegetation–climate anomalies dynamics, especially in the targeted area, and offers a clear idea of the biotic and abiotic stresses that are the response to temporal vegetation syndrome (Fig. 2.1a).

Theoretically, we have modified the target area based on the climate gradient with Köppen classification to estimate the SPIE dataset (Table 2.1). For instance, in the category *BWk* and *Csa* are located the following regions: Lebap (Turkmenistan)

[1] Mean annual precipitation (70%) accumulated during winter period.

Table 2.1 Köppen climate symbols and related criteria for Central Asia (modified after Peel et al. 2007)

1st	2nd	3rd	Description	Regions	Criteria[a]	SPIE selected category
B			Arid		$MAP < 10 \times P_{threshold}$	
	W		–Desert	Uzb,Trk,	$MAP < 5 \times P_{threshold}$	
	S		–Steppe	Kzk, Uzb, Trk	$MAP \geq 5 \times P_{threshold}$	BSk-Ulytau, Naryn
		h	Hot	Trk, Uzb	$MAT \geq 18$	
		k	Cold	Trk, Uzb, Kzk	$MAT < 18$	BWk-Lebap, Navoi, GBAR
C			Temperate		$T_{hot} > 10$ & $0 < T_{cold} < 18$	
	s		–Dry summer		$P_{sdry} < 40$ & $P_{sdry} < P_{wwet}/3$	
	w		–Dry winter		$P_{wdry} < P_{swet}/10$	
	f		–Without dry season		Not (Cs) or (Cw)	
		a	Hot summer	Taj	$T_{hot} \geq 22$	Csa-Lebap, Navoi
		b	–Warm summer		Not (a) & $T_{mon10} \geq 4$	
		c	–Cold summer		Not (a or b) & $1 \leq T_{mon10} < 4$	
D			Cold		$T_{hot} > 10$ & $0 < T_{cold} \leq 0$	
	s		–Dry summer	Uzb, Taj, Krg, Kaz	$P_{sdry} < 40$ & $P_{sdry} < P_{wwet}/3$	
	w		–Dry winter		$P_{wdry} < P_{swet}/10$	
	f		–Without dry season		Not (Ds) or (Dw)	
		a	–Hot summer	Kaz, Krg	$T_{hot} \geq 22$	Dsa-GBAR
		b	–Warm summer	Krg	Not (a) & $T_{mon10} \geq 4$	
		c	–Cold summer		Not (a, b or d)	
		d	–Very cold summer		Not (a or b) & $T_{cold} < -38$	

[a]*MAP* mean annual precipitation, *MAT* mean annual temperature, T_{hot} temperature of the hottest month, T_{cold} temperature of the coldest month, T_{mon10} number of months where the temperature is above 10°, P_{dry} precipitation of the driest month, P_{sdry} precipitation of the driest month in summer, P_{wdry} precipitation of the driest month in winter, P_{swet} precipitation of the wettest month in summer, P_{wwet} precipitation of the wettest month in winter, $P_{threshold}$ varies according to the following rules (if 70% of MAP occurs in winter then $P_{threshold} = 2 \times MAT$; if 70% of MAP occurs in summer then $P_{threshold} = 2 \times MAT + 28$, otherwise $P_{threshold} = 2 \times MAT + 14$). Summer (winter) is defined as the warmer (cooler) 6-month period of ONDJFM and AMJJAS

Table 2.2 Summary of input datasets for parameterizing methodology of kriging

Data	Indices	Temporal scale	Time span (extracted)[a]	Spatial scale	Data source
NDVI	Vegetation	Bimonthly	1982–2015	8 km	AVHRR-GIMMS (NDVI 3g)
SPIE	Drought	Monthly	1982–2015/1950–2017	0.5×0.5^0	SPIEbase
Average temperature	Climate	Monthly	1901–2015/1982–2015	0.5×0.5^0	CRU-TS (ver. 4)
Average precipitation	Climate	Monthly	1901–2015/1982–2015	0.5×0.5^0	CRU-TS (ver. 4)

[a]For simulation data, and for kriging methodology it has been extracted years between 1982 and 2015, originality data available or occupied past (before 1982) and present (after 2011) periods

and Navoi (Uzbekistan); in *BWk* are Kyzylorda (Kazakhstan) and GBAR (Tajikistan); and in the *BSk* category are Ulytau (Kazakhstan), Naryn (Kyrgyzstan); all estimated by their past and ongoing occurrences.

2.2.2.1 Datasets and Methods

To determine whether and how vegetation dynamics in Central Asian drylands are associated with climate patterns and NDVI, we used bimonthly 8-km GIMMS AVHRR data (1982–2015), and compared with time series data [CRU TS (v4.23)] for precipitation and temperature effects (1982–2015) during the selected period of time (Jones and Harris 2008) and calibrated with SPIE time series data (1982–2017). In Table 2.2, a detailed explanation is provided for each dataset and resolution scales. However, correction of the forecasting (prediction map) was estimated for the period 1982–2015 because of the availability of the NDVI dataset for this period. Originally, some drivers have longer periods, such as SPIE (1950–2017) and CRU-TS (1901–2015). Environmental variables (temperature, precipitation, and NDVI; SPIE) have been analyzed with the geostatistics method: a detailed description is illustrated on the flowchart (Fig. 2.4).

Environmental variables are indicated as a certainty dataset because of the utilization of various factors for estimation parameters and their dependency on each other. To account for surface biophysical properties of various habitats (Fig. 2.1a, b) and to assess the temporal movement dynamics of vegetation patterns in these cold desert and semi-desert ecosystems, we utilized a simple kriging methodology that was developed to classify further the vegetation index, which is identifying as index certainty associated factors (Prec/Temp/NDVI/SPIE) influencing the solid earth.

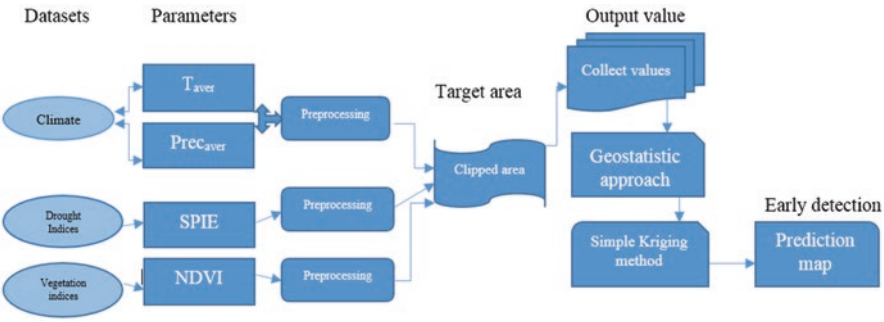

Fig. 2.4 Flowchart represents the steps of composing datasets and data processing for target area explored among Kazakhstan, Kyrgyzstan, Tajikistan, Turkmenistan, and Uzbekistan

2.2.2.2 Climatic Variables

The CRU time series (0.5 × 0.5 degree) grid datasets were extracted for 1982–2015 to assess month-by-month variation for climate/precipitation on a larger scale (Harris et al. 2014). Mapping climatic and precipitation data need to consider that some gaps are available during/after 1982–1991; it is clear that after collapse of the USSR some stations have ceased their missions, affecting the quantity of data. Climate data visualized over this time show quite high temperatures (since 1982–1992), which later becomes stabilized (after 2000).

2.2.2.3 A Drought Index: The Standardized Precipitation-Evapotranspiration Index (SPEI)

The SPEI is a multiscalar drought index based on climatic data and estimated based on the CRU-TS dataset. The SPEI-drought monitor offers near real-time information about drought conditions at the global scale, with a 0.5° spatial resolution and a monthly time resolution. Available to be downloaded on the following https://climatedataguide.ucar.edu/data-type/climate-indices/drought/spei, the SPEI is obtained from the monthly climatic water balance [precipitation minus reference evapotranspiration, $\left(ET_{0^-}\right)$], which is adjusted using a three-parameter log-logistic distribution. The values are accumulated at various time scales and converted to standard deviations with respect to average values (Vicente-Serrano et al. 2015a, b). The calibration period for the SPEI is January 1950 to December 2017 (last access: March 2018). For long-term analysis and calculation of selected target zone (Central Asia) habitats, we have scaled with a 1-month period with the same available calibration time (1950–2017) and as requested a robust understanding of the interrelations of the drought rankings in Central Asia (Fig. 2.5b). Determining the onset and duration of drought conditions with respect to normal conditions in a variety of natural and managed systems such as crops is best suited for drought monitoring and early warning purposes. Within this purpose, we have explored five countries

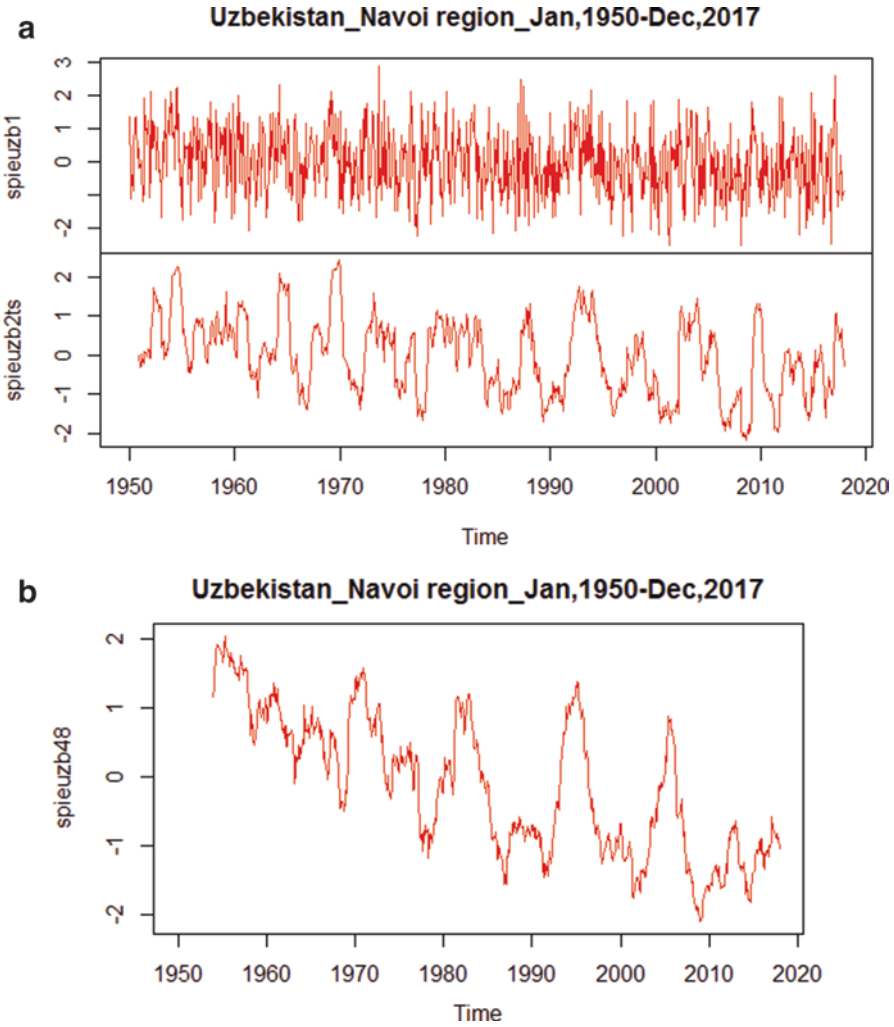

Fig. 2.5 Main drought episodes in Uzbekistan for Navoi region as occurred by SPIE dataset: monthly and annually distributions of drought (**a**) and 4 years cycling the drought trends (**b**). (**a**) SPIE_1: monthly and SPIE_12: annual dataset for Uzbekistan (Jan 1950–Dec 2017). (**b**) SPIE_48: counting and averaging for each 4 years

separately to visualize SPIE ratings for the past 70 years, within this purpose to be able compare with NDVI values (1982–2015). The process is determined by applying R programming language (within "spie" dataset) and this set of function (dataset) computing SPIE dataset (Beguería et al. 2014) and following the classical approximation as estimated and updated by Abramowitz and Stegun (1965).

$$\mathrm{SPEI} = W - \frac{C_0 + C_1 W + C_2 W^2}{1 + d_1 W + d_2 W^2 + d_3 W^3}, \tag{2.1}$$

where

$$W = \sqrt{-2\ln(P)} \quad \text{for} \quad P \leq 0.5 \tag{2.2}$$

and P is the probability of exceeding a determined d value, $P = 1 - F(x)$.

If $P > 0.5$, then P is replaced by $1 - P$ and the sign of the resultant SPEI is reversed (Vicente-Serrano et al. 2010). The constants are $C_0 = 2.515517$, $C_1 = 0.802853$, $C_2 = 0.010328$, $d_1 = 1.432788$, $d_2 = 0.189269$, and $d_3 = 0.001308$. The equations are cited at http://spei.csic.es/home.html and upgraded by Vicente (Vicente-Serrano et al. 2010). An R package is available for calculating the SPEI from user-selected input data using either the Thornthwaite, Penman-Monteith, or Hargreaves methods. For mapping, we have used the SPIEbase with based on NetCDF format, what was upgraded after the CRU-TS dataset.

2.2.2.4 Vegetation Indices: Normalized Difference Vegetation Index (NDVI)

In the framework, datasets from the Global Inventory Monitoring and Modeling System (GIMMS) project are carefully assembled from different AVHRR sensors and account for various deleterious effects, such as calibration loss, orbital drift, and volcanic eruptions (Tucker and Pinzon 2013). Bimonthly with 8-km resolution GIMMS AVHRR-NDVI3g data (1982–2015) were utilized to analyze NDVI (vegetation) status for Central Asia. The vegetation models were developed and generated subsequently with using climatic variables [temperature (average) and precipitation (average)] and drought index (SPIE) and NDVI, respectively, in the same period for kriging methodology approaches.

2.2.2.5 Probalistic Methods to Predict and Monitor Further Status of Landscapes (Kriging)

The assessment based on application of satellite images (NDVI 3g) with certainty datasets ($Prec_{monthly}$/$Temp_{monthly}$/$SPIE_{monthly}$) was developed on the base requirements of geostatistics to provide probability of further status within prediction of negative patterns or land degradation areas in Central Asia. Within this aim, we have used the kriging method with variograms to detect degradation categories, and calculated several environmental variable parameters for better understanding of forthcoming years conditions resulting from scarcity/limitations of water resources and fast land triggering issues. A major factor also is a warming temperature that influenced mismanagement basins (abiotic factors) by the overuse of its tributary rivers. More accuracy was found when we utilized geostatistical methodology for a large dataset (the territory of Central Asia is ~4,002,900 km^2). Another method using Empirical Bayesian Kriging (EBK) is more suitable, and also this methodology is reliable for

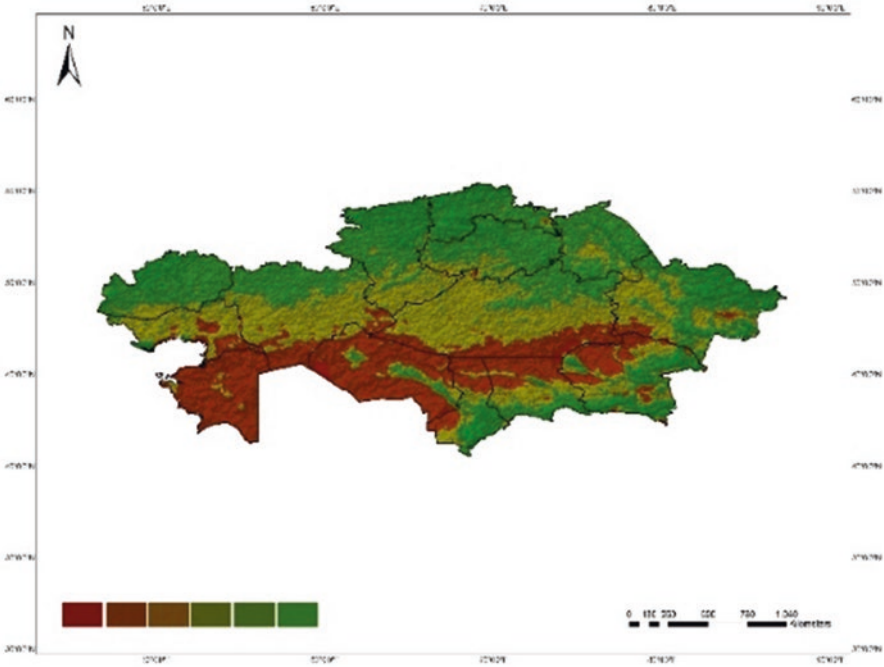

Fig. 2.6 SPIE-based mapping of drought episodes in Kazakhstan (1950–2017)

interpolation of the target area. This methodology provides greater accuracy for estimating forest or cropland status (areas with a high greenness index), but for drylands low to moderate vegetation values are better simulated with the kriging (simple and ordinary) method (see results on Figs. 2.6 and 2.7). The predicted map with the kriging dependence terms visualized more realistic means to classify vegetation patterns (low values of NDVI) and particularly with application of SPIE datasets. A probalistic method is required to provide information on prediction uncertainty limits and the choice of interpolators to statistical ones.

2.3 Results

We are intending to demonstrate the SPIE dataset as responsible for loss of energy in the balance (vegetation patterns) resulting from an outgoing high ET_0 in the drylands of CA. On the open rangelands, incoming high radiation is the source of high ET_0 ratings. Centrally, Turkmenistan and Uzbekistan, and partly Tajikistan (western), and farthest in Kazakhstan (southern side), this is a main source of losing a high energy balance from vegetation patterns.

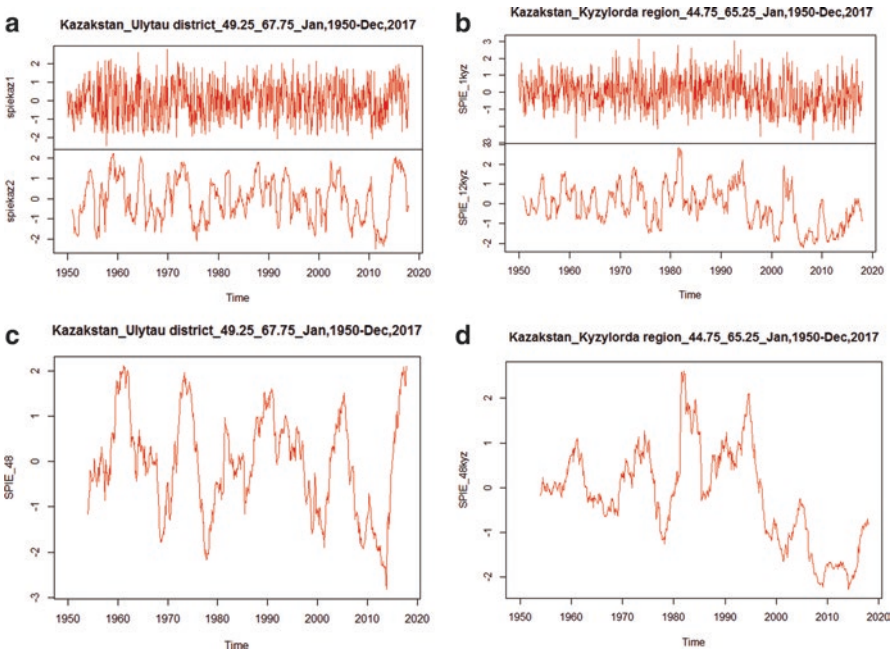

Fig. 2.7 Main drought episodes in Kazakhstan for Ulytau and Kyzylorda regions occurred by SPIE dataset (**a**, **b**) monthly and annual distributions of drought and (**c**, **d**) 4 years cycling of drought trends. (**a**) SPIE_1: Monthly and SPIE_12: annually dataset for Ulytau district, Kazakhstan (Jan 1950–Dec 2017). (**b**) SPIE_1: Monthly and SPIE_12: annually dataset for Kyzylorda, Kazakhstan (Jan 1950–Dec 2017). (**c**) SPIE_48: counting and averaging for each 4 years in case of Ulatau, Kazakhstan. (**d**) SPIE_48: counting and averaging for each 4 years in case of Kyzylorda, Kazakhstan

2.3.1 Long-Term Trends of SPIE Data (1950–2017) for Selected Areas

Mapping and determining monthly trends, annually drought variability (1950–2017) and multiplicative year (each 4 years) of trends (1950–2017) was found in targeted areas with positive and negative trends of SPIE (ratings between 2 and −2). Drought categories were derived based on Charusombat and Niyogi (2011) and modified after Ta et al. (2018) (listed in Table 2.3). Inserted shapes of the mapping part indicated alterations in the selected regions (green is normal, red is negative). Trends modified and updated on the database SPIEbase 2, and observation, show evidence that a drought is triggering the land degradation process, and that long-term drought is stressful for crops, explaining the major degradation trends (Figs. 2.5, 2.8, 2.9, 2.10, and 2.11).

Table 2.3 Standardized Precipitation-Evapotranspiration Index (SPEI) category for estimation of drought variety

Drought ranking	SPIE category
Extreme drought	SPEI ≤ -2.0
Severe drought	$-1.99 <$ SPEI < -1.5
Moderate drought	$-1.49 <$ SPEI ≤ -1.0
Mild drought	$-0.99 <$ SPEI ≤ -0.5
Non-drought	SPEI ≥ -0

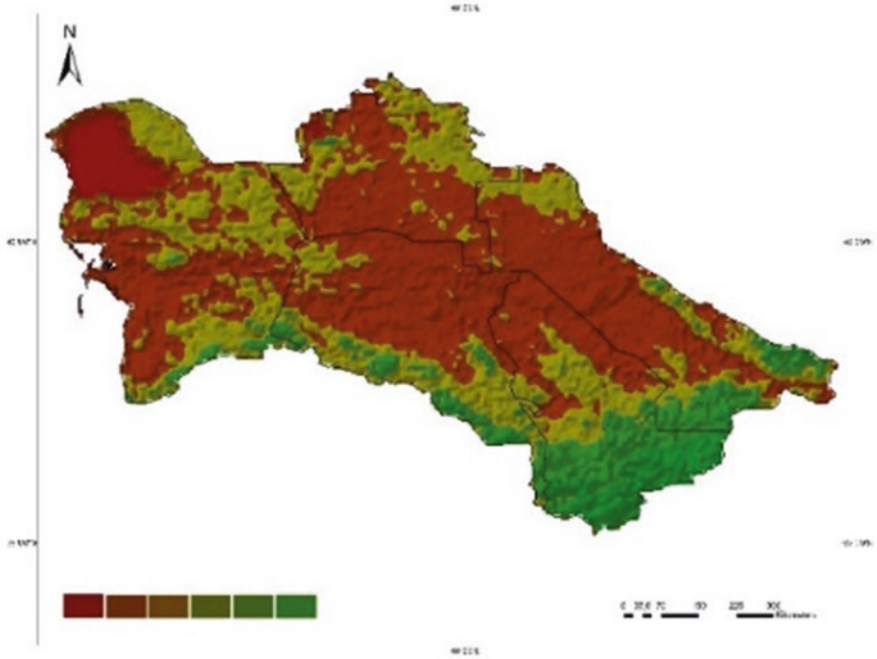

Fig. 2.8 SPIE-based mapping of drought episodes in Turkmenistan (1950–2017)

The main drought episodes occurred in the late 1950s, and unfavorable occasions were observed in late 2010 for all five countries within six regions. For the time series dataset we have added extra basic requirements for better understanding the anomaly in decades of time (Y coordinate values reached ≥ -1 and ≥ -2, which means a serious drought period of years or month in the region, and 0 trends mean no changes during the annual period), and the mapping part is inserted with shapes where time series are analyzed on pixel-based coordinate data (Figs. 2.4, 2.12, 2.13, 2.14, and 2.15). We are quickly able to see a high drought period for each 4 years (Figs. 2.4, 2.12, 2.13, 2.14, and 2.15, right side, with trends); 48 SPIE datasets were analyzed, demonstrating the averaging drought value for each 4 years based on average values.

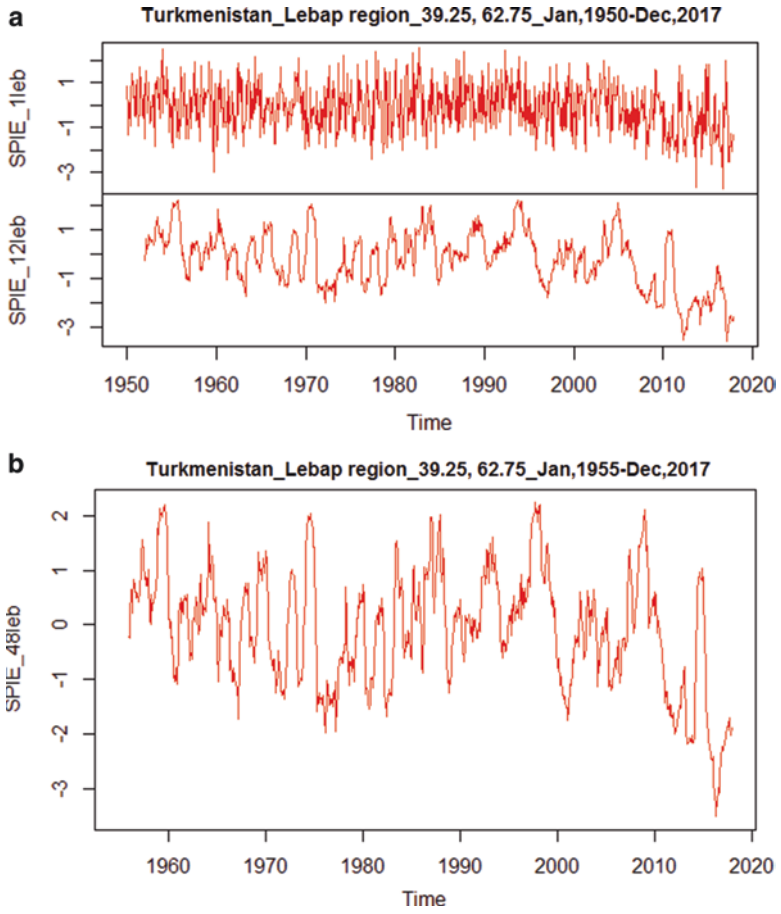

Fig. 2.9 Main drought episodes in Turkmenistan for Lebap region as occurred by SPIE dataset: monthly and annual distributions of drought (**a**) and 4 years cycling of drought trends (**b**). (**a**) SPIE_1: Monthly and SPIE_12: annually dataset for Lebap region, Kazakhstan (Jan 1950–Dec 2017). (**b**) SPIE_48: counting and averaging for each 4 years in case of Lebap, Turkmenistan

2.3.1.1 Uzbekistan

Drought is a common occasion in Central Asia, especially for the parts of Turkmenistan and Uzbekistan, and is more influenced by climate or landscape distributions. for the part of Uzbekistan, the Navoi region was selected (coordinates 40°25′–65°25′), located in the middle zone of the country. Originally, the area was classified as cold desert zone (BWk, Koeppen classification), and drought frequency is the usual issue on this area because of high temperature and low precipitation. However, how frequently drought is observed in this area is demonstrated in

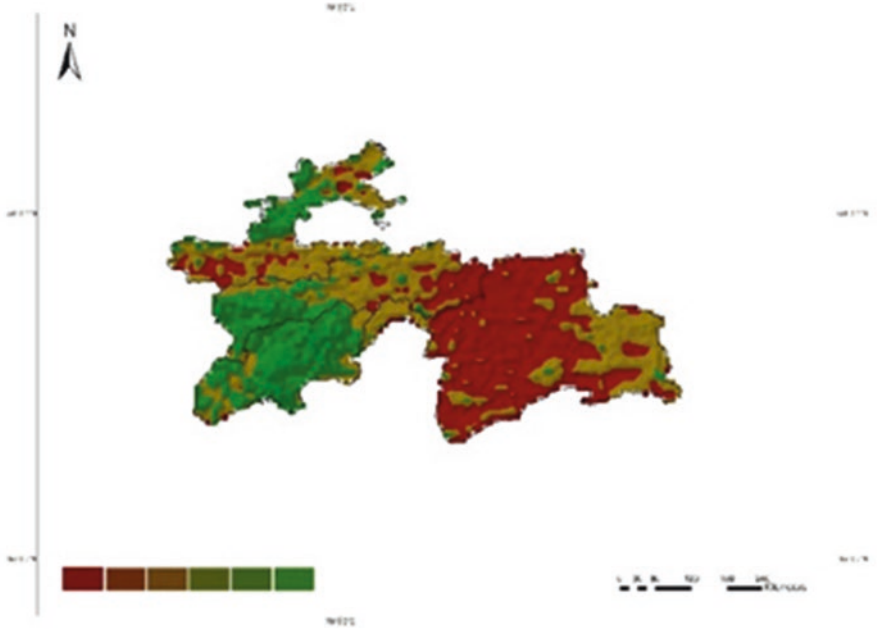

Fig. 2.10 SPIE-based mapping of drought episodes in Tajikistan (1982–2015)

Fig. 2.16, and for each 4 years it possible to observe strong droughts that correspond to above >−2 (Fig. 2.16).

Based on annual data, the strongest droughts were observed in the middle 1960s and the early 1970s. In past decades, during the 2000s, 2009 was recorded as the strongest one (Fig. 2.4a, left side). The importance of this selected point is related to estimating regions that are not a source to water basins and to get an idea about drought occurrences for areas far away from water resources. Based on vegetation classification, it is classified as *Artemisia* spp., a shrubland zone and therefore our first point (Navoi region) classified as being the desert type of vegetation (Fig. 2.1b).

2.3.1.2 Kazakhstan

Almost 70 years observation (1950–2017) estimated the strong droughts in Ulytau, and the last years negatively with further negative trends for Kyzylorda region (Fig. 2.12), whereas the mapping part shows that the northern part illustrated a positive scale (low drought) and the middle of the country a moderate level (values) of drought (Fig. 2.8). The difference between Ulytau and Kyzylorda is related to an accumulation on minimum values of drought indices, such as strongest or peak of drought (max >−2) observed in the Kyzylorda region (see mean values with minus),

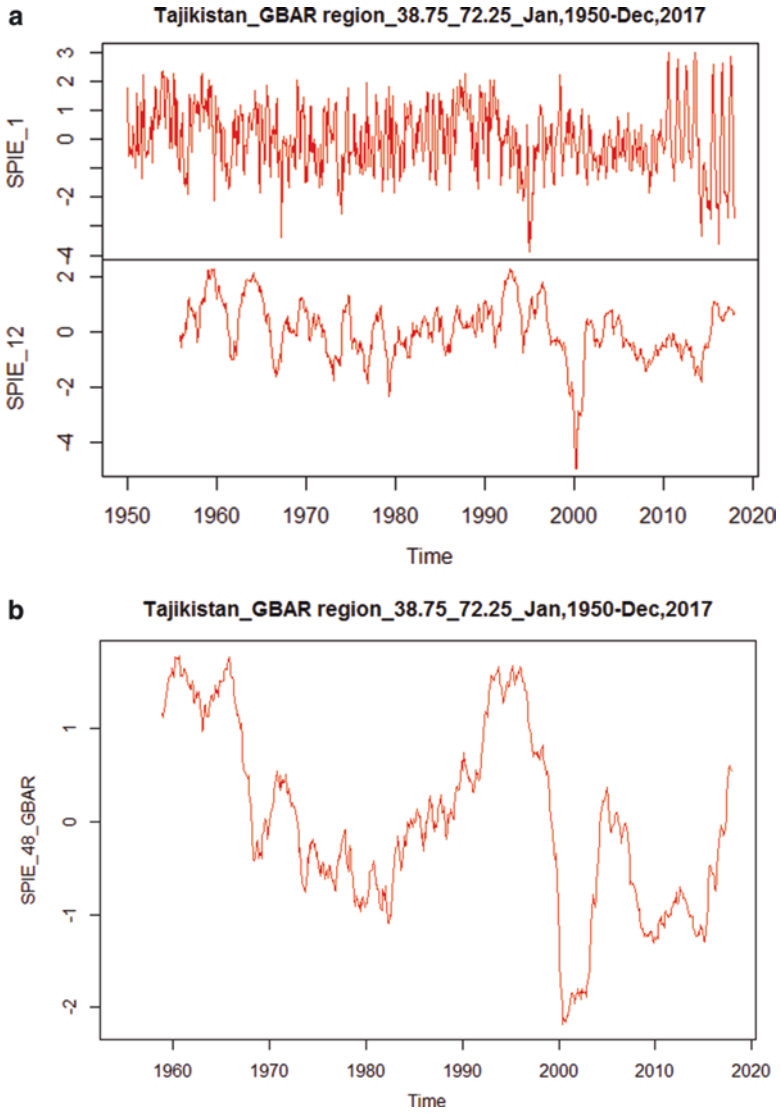

Fig. 2.11 SPIE based mapping of drought episodes in Tajikistan (1982–2015). The selected point located on the GBAR region, the area where covered partly with mountains. The main drought episodes in Tajikistan for Lebap region occurred by SPIE dataset, (**a**) monthly and annually distributions of drought and (**b**) 4 years cycling the drought trends. (**a**) SPIE_1: Monthly and SPIE_12: annually dataset for GBAR region, Tajikistan (Jan 1950–Dec 2017). (**b**) SPIE_48: counting and averaging for each 4 years in case of GBAR, Tajikistan

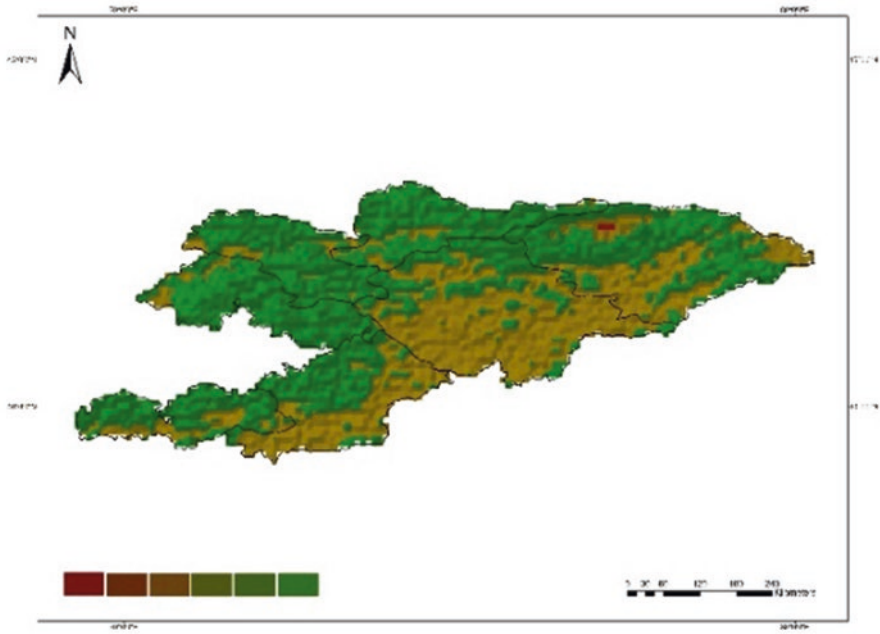

Fig. 2.12 SPIE-based mapping of drought episodes in Kyrgyzstan (1982–2015)

while frequently a positive median among null (no droughts) in Ulytau occurred with greater frequency.

2.3.1.3 Turkmenistan

The main drought episodes in Turkmenistan occurred in the past decades; also, SPIE_48 for the Lebap region (Fig. 2.13a); Fig. 2.13b illustrates that among 4 years calculations the strongest one is between 2013 and 2017.On the monthly dataset, the strongest or extreme strong drought values are illustrated between 2015 and 2017 (Fig. 2.13b).

2.3.1.4 Tajikistan

In this area, the last years are categorized mostly with strong drought trends that reached SPIE >−4 in some months of 2010–2017 (Fig. 2.14a, b), whereas in further upcoming years for the GBAR region might be also observed no drought trends as counted by linearity forecasting (Fig. 2.14c). The strongest SPIE >−3 is observed in

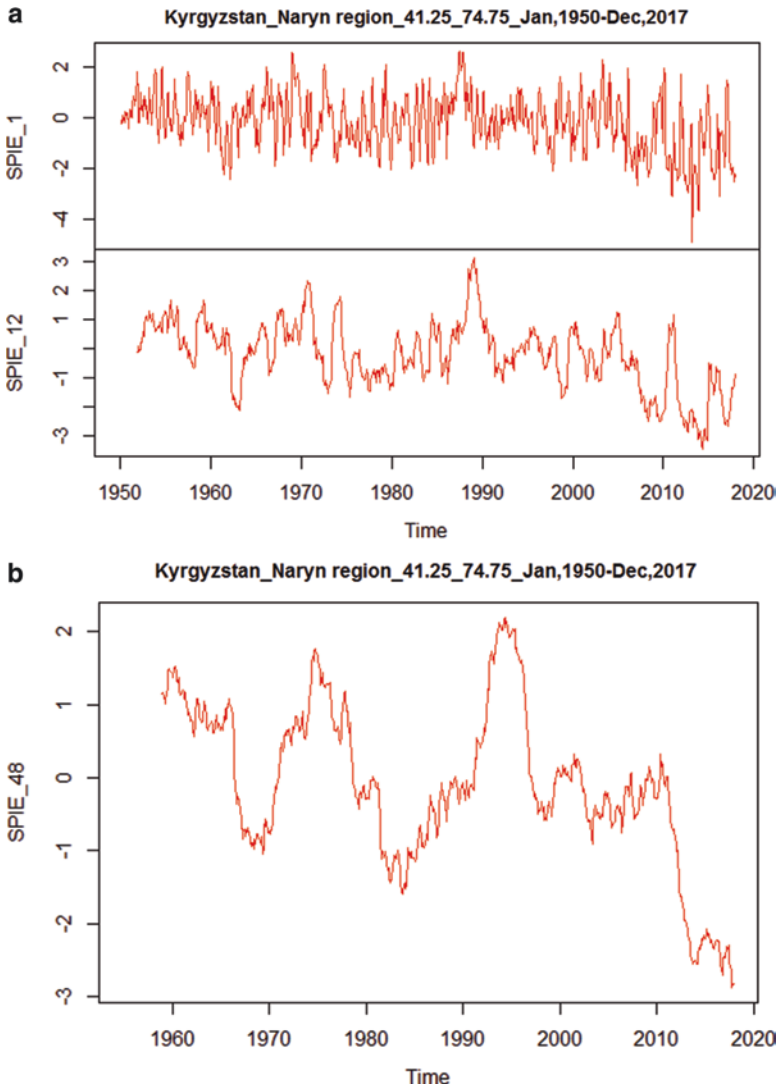

Fig. 2.13 The main drought episodes in Kyrgyzstan for Naryn region occurred by SPIE dataset, (**a**) monthly and annually distributions of drought and (**b**) 4 years cycling the drought trends. (**a**) SPIE_1: Monthly and SPIE_12: annually dataset for Naryn region, Kyrgyzstan (Jan 1950–Dec 2017). (**b**) SPIE_48: counting and averaging for each 4 years in case of Naryn, Kyrgyzstan

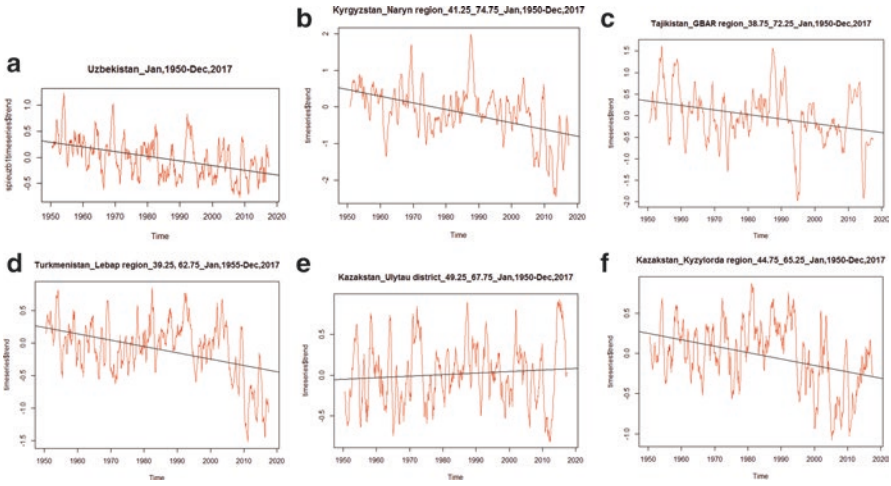

Fig. 2.14 Annual drought trends in Central Asia (1950–2017) and linear prediction to 2020. (**a**) Annual drought trends in Uzbekistan (1950–2017) and linear prediction to 2020. (**b**) Annual drought trends in Kyrgyzstan (1950–2017) and linear prediction to 2020. (**c**) Annual drought trends in Tajikistan (1950–2017) and linear prediction to 2020. (**d**) Annual drought trends in Turkmenistan (1950–2017) and linear prediction to 2020. (**e**) Annual drought trends in Ulytau, Kazakhstan (1950–2017) and linear prediction to 2020. (**f**) Annual drought trends in Kyzylorda, Kazakhstan (1950–2017) and linear prediction to 2020

the 2000s, while annually is mostly on positive level (Fig. 2.14d, e). According to 4-year estimations, the period of 2010 was also a moderate drought period (Fig. 2.14f).

2.3.1.5 Kyrgyzstan

In this area, past years show mostly strong drought trends, and it is estimated that it reached SPIE >−3 in some months after 2010 (Fig. 2.15); for further upcoming years for the Naryn region, drought trends might be also observed (as SPIE >−1) as counted by linearity forecasting (Fig. 2.17b). Results indicated that negative trends of drought severity index (red color) are related to low accumulation of NDVI values, and a positive drought index included high or moderate values of NDVI, as in Central Asia, where high values of NDVI ranged between 0.35 and 0.50. Kyrgyzstan is dominant with high values of NDVI, and no drought according to drought mapping (Fig. 2.11), and mostly positive trends of drought severity index indicated in Naryn region (except for 2015).

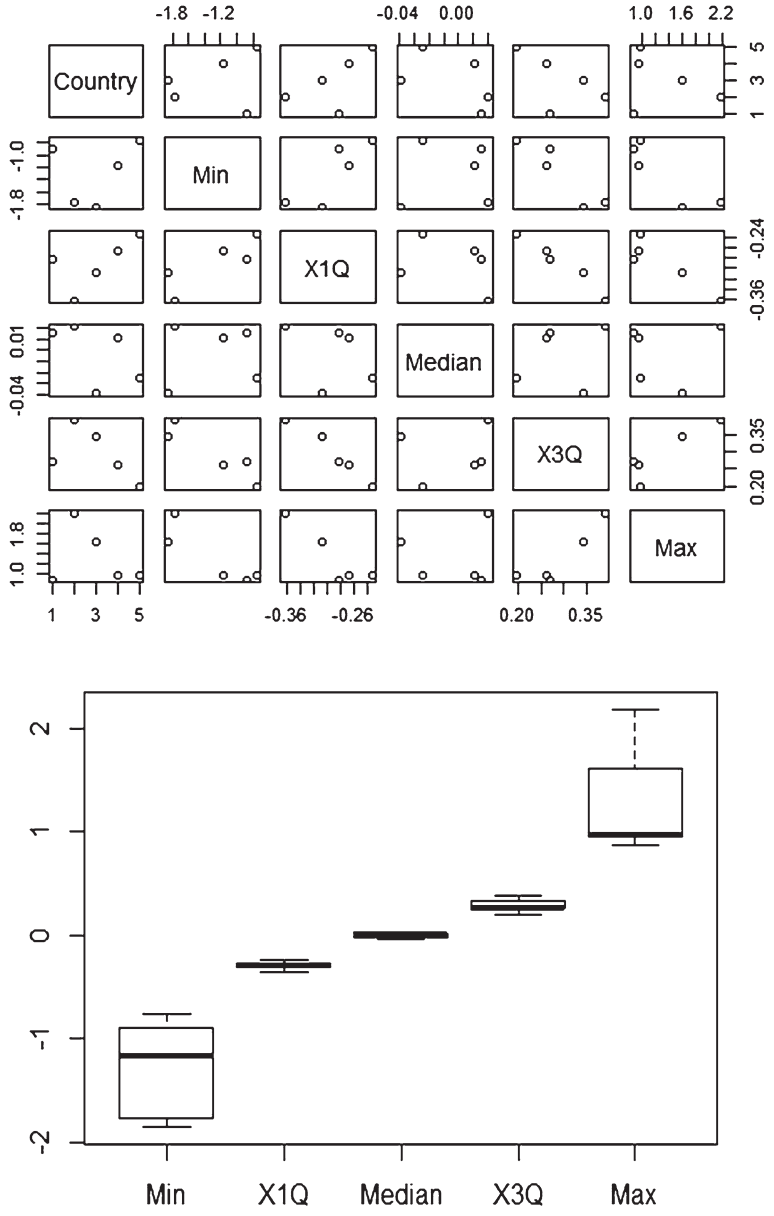

Fig. 2.15 Scatterplot and boxplot analysis for drought residuals in five areas of Central Asia. On the column level: *1* Uzbekistan, *2* Kazakhstan, *3* Kyrgyzstan, *4* Turkmenistan, *5* Tajikistan

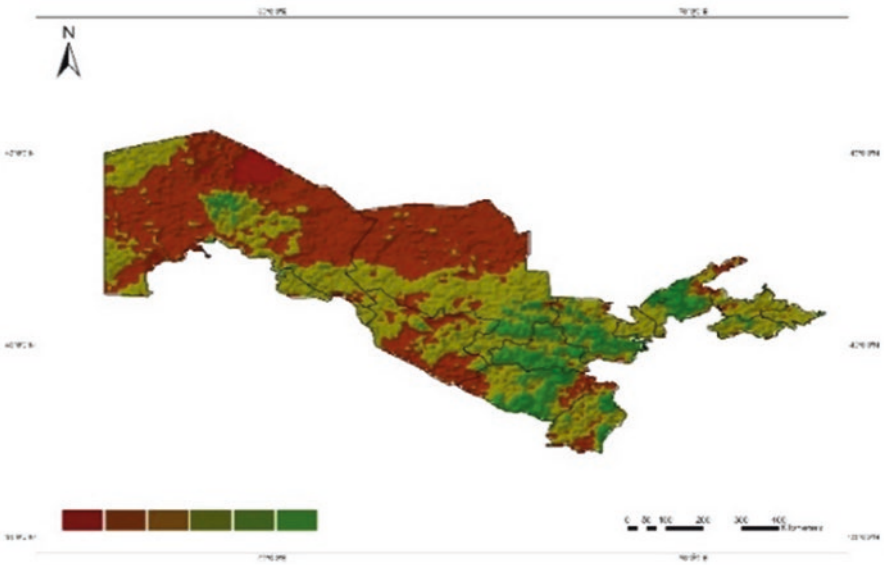

Fig. 2.16 Mapping annual SPIE dataset for Uzbekistan based on available period (1950–2017)

This is a preliminary conclusion of results, and all highlights are a complexity of drought activity processes to describe generally.

2.3.2 Summary About Droughts for Central Asia

On the basis of the results, each country has observed a very extreme drought period at least two times during the observation period (1950–2017); occasionally, it is not similar for each country in addition to region. However, mostly the strongest drought was observed for 2010 in all countries. These phenomena, which vary with time, related to develop a particular span of time. As demonstrated results and drought coefficients, the negligible condition is observed in Lebap (Turkmenistan) and Ulytau (Kazakhstan) regions. Based on observed results, the SPEI is a good indicator to predict further drought anomalies or alternatively to be able develop crop failure or less productive zones under a statistical approach (Table 2.4).

2.3.3 Statistical Description of Annual Trend Analysis of Droughts and Their Residuals

The selected method outputs describes the results of drought on annual trends based on monthly dataset. The seasonal fluctuations in a time series can be contrasted with cyclical patterns (see on top) (Tables 2.5, 2.6, and 2.7). To handle seasonality with amplitude and phase are a linear regression for drought trends and calculated with

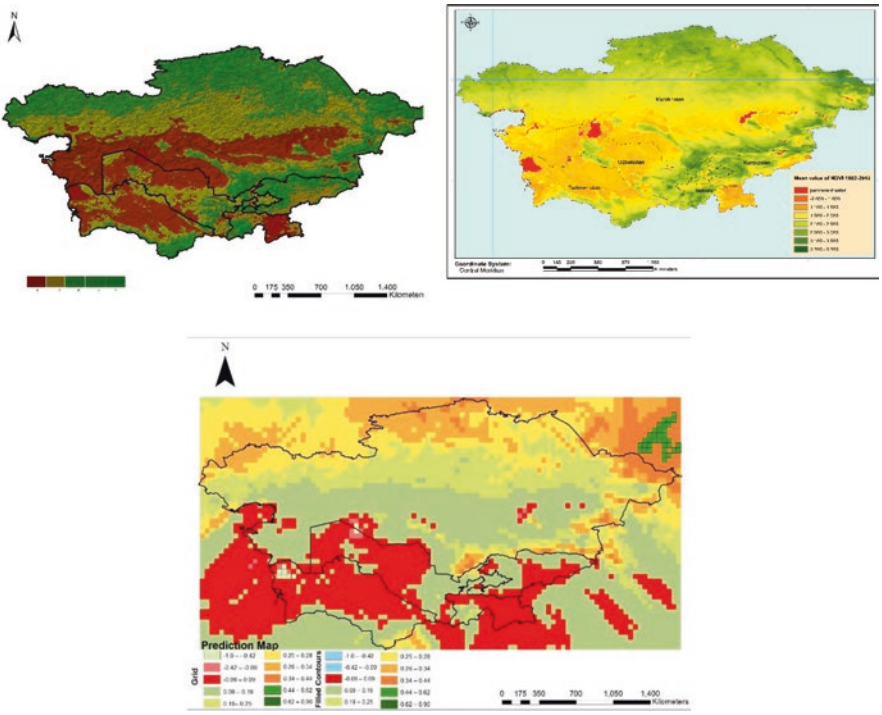

Fig. 2.17 Mapping prediction standard error on base kriging results (prediction made on the basis of regression equation). Results indicated similarity of SPIE index with Köppen classification (**a**, **b**) and average annual NDVI values (**c**) and prediction map with simple kriging method (**d**). (**a**) Drought indices of SPEI (1982–2015) and identified similarity Köppen classification. (**b**) NDVI values (1982–2015) determined on the high evaporation zones with low vegetation values. (**c**) Prediction map for changes of vegetation indices in Central Asia. A high loss of vegetation indices is indicated in the southern territories and occupied Turkmenistan, Tajikistan, and Uzbekistan. Red color is modified as early drought detection zones

Table 2.4 Basic statistical description monthly available SPIE dataset in the part of Uzbekistan (1957–2017)

Minimum	1st quarter	Median	Mean	3rd quarter	Maximum
−2.17	−0.83	−0.01	−0.05	0.65	2.42

Table 2.5 Basic statistical description of monthly available SPIE dataset in the part of Uzbekistan (1957–2017)

Ulytau					
Minimum	1st quarter	Median	Mean	3rd quarter	Maximum
−2.415740	−0.731258	0.000685	0.015693	0.748020	2.764420
Kyzylorda					
Minimum	1st quarter	Median	Mean	3rd quarter	Maximum
−2.78183	−0.73523	−0.04258	−0.02281	0.66500	3.15759

Table 2.6 Basic Statistical description monthly available SPIE dataset in the part of Uzbekistan (1957–2017)

Min.	1st Qu.	Median	Mean	3rd Qu.	Max.	NA's
−3.89508	−0.77346	−0.07035	−0.01224	0.76384	2.99554	1

Table 2.7 Basic statistical description monthly available SPIE dataset in the part of Uzbekistan (1957–2017)

Min.	1st Qu.	Median	Mean	3rd Qu.	Max.	NA's
−4.89750	−0.87012	−0.07526	−0.15617	0.61815	2.64364	2

decomposition method from time series analysis series. As we have seen, for the six cases (selected target areas), the annual trend values ranged between −2 and 2 (as minus "drought," with plus "low drought"). Based on residuals and forecasting in further drought status (Fig. 2.17) illustrates that only in the Ulytau region, Kazakhstan will have less drought, or positive trends will have affirmed it. Other resting areas are shown with negative trends (descending line); especially, Turkmenistan (Lebap) and Kazakhstan (Kyzylorda) will be stronger than other areas. Other statically available data for residuals is illustrated in Tables 2.8 and 2.9. The following residual analysis of annual drought trends is based on the monthly dataset accounted for each region (Table 2.9) and the following abbreviations meaning the value: for example, for Uzbekistan, minimum (Min): Min = −0.76; first quartile (1Q):1Q = −0.23; Median (Med): Med = −0.02; Third Quartile (3Q):3Q = 0.19; and Maximum (Max): Max = 0.98.

2.3.4 Resilience of Ecosystem and an Assessment of the Consequences of Current Factors for Vegetation Trends

Drought-persistent periods are various and dependent on annual rainfall data, and the following nonsmoothing parameters are developed for irregular patterns of precipitation and drought trends. Obviously, temperature raising trends are affected on Central Asian drylands and our preliminary studies has proved that land degradation is directly linked to Central Asian habitats. Using a semi-variogram as a model, new data are unconditionally simulated at each of the input locations in the subset; in the case of the large number of datasets are plotted together and measured for prediction. The indicator prediction values are calculated using the semi-variogram modeled from the binary (0–1) data, the creation dataset based on indicator transformations of original data (Prec/Temp/NDVI/SPIE).

Cross-validation sequentially omits a point and calculates indicator prediction values for each dataset. The simulating semi-variogram (Fig. 2.18a) with the cer-

Table 2.8 Drought coefficients in selection regions of Central Asia

Countries	Intercepts	Estimate	St. error	*t*-value	Pr(>|*t*|)	Multiple *R*-squared	Adjusted *R*-squared	*p*-value
Uzbekistan	sin(2* π*drought)	17.92	1.13	15.85	<2e−16 ***			
Uzbekistan	cos(2* π *drought)	−0.01	0.00	−15.86	<2e−16 ***	0.2387	0.2378	<2.2e−16
Kyrgyzstan	sin(2* π *drought)	35.99	2.26	15.86	<2e−16 ***			
Kyrgyzstan	cos(2* π *drought)	−0.01	0.00	−15.92	<2e−16 ***	0.2406	0.2397	<2.2e−16
Tajikistan	sin(2* π *drought)	20.76	2.14	9.668	<2e−16 ***			
Tajikistan	cos(2* π *drought)	−0.01	0.00	−9.673	<2e−16 ***	0.10	0.10	<2.2e−16
Turkmenistan	sin(2* π *drought)	19.31	1.43	13.46	<2e−16			
Turkmenistan	cos(2* π *drought)	−0.01	0.00	−13.52	<2e−16	0.1857	0.1847	<2.2e−16
Kazakhstan(Ulytau)	sin(2* π *drought)	−3.74	1.35	−2.76	0.00584 **			
Kazakhstan(Ulytau)	cos(2* π *drought)	0.00	0.00	2.77	0.00563 **	0.01	0.01	0.005631

Signif. codes: 0 '***'; 0.001 '**' ;0.01 '*'; 0.05 '.' ; 0.1 ' ' ; 1

Table 2.9 Summary for residual analysis of monthly drought values and outputs between trends and seasonality

Country	Min	1Q	Median	3Q	Max
Uzbekistan (Navoi)	−0.75964	−0.23210	−0.02444	0.19754	0.98208
Kazakhstan (Ulatau)	−0.88626	−0.28184	0.01544	0.27061	0.87385
Kyrgyzstan (Naryn)	−1.76631	−0.36260	0.02083	0.39100	2.18888
Turkmenistan (Lebap)	−1.1657	−0.2658	0.0114	0.2616	0.9576
Tajikistan (GBAR)	−1.85109	−0.30753	−0.03922	0.34162	1.61468

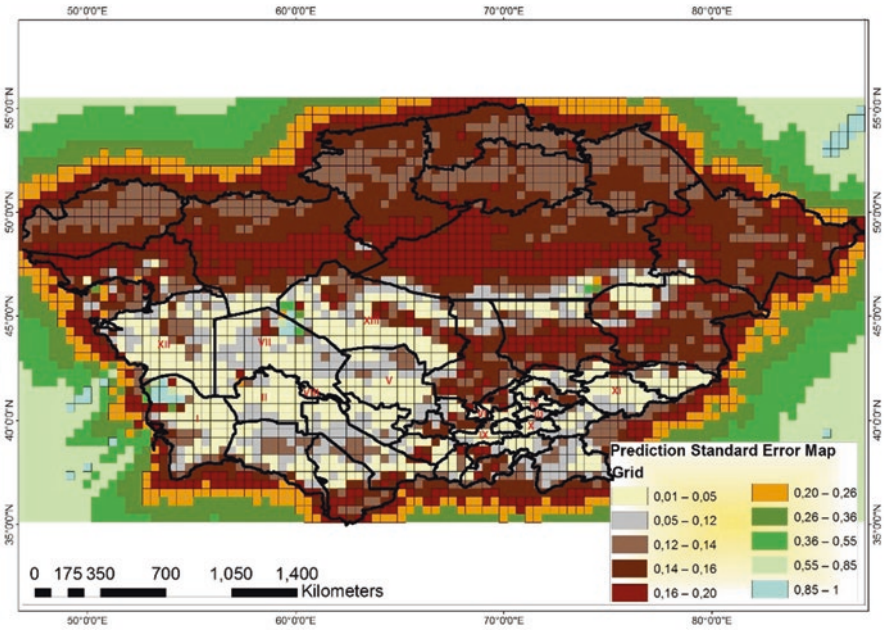

Fig. 2.18 Mapping prediction standard error on base kriging results (prediction made on the basis of regression equation)

tainty associated (*Prec/Temp/NDVI/SPIE*) dataset is constructed by calculating half the average squared difference of the values of all pairs (NDVI vs. Prec, SPIE vs. Temp) of measurements at locations separated by a given distance h (h*10^{-1}) and plotted as y (y*10^{-2}) against the separation distance h (Fig. 2.18a). In reality, it means the uncertainty prediction after measuring level 0.636 is various or diffused and a randomly occupied measured distance (Fig. 2.18b). Because of the accumulation of low vegetation as sparse vegetation, after 0.636 it was hard to predict after this level and variations of the dataset are occasionally diffused. An inserted shape indicates dominant values for these zones that are tightly accumulated and less extending (more stabilized) in both sides between planks.

The number of lags 12 monthly, lag size >12 for datasets, defines the weights that determine the contribution of each observed data point to the prediction of new values at unsampled locations. The selected number 12 is indicated as monthly contributions and their delay effects. This is an effective way to acquire vegetation covers because they are time consuming, and curvature (Fig. 2.18a) effects to lags are very small and averaged datasets (blue crosses) are nonsignificant to the semivariogram. As illustrated in Fig. 2.18a, the semi-variogram is estimated from data to make optimal prediction among various distances (dataset as frequently diffusion from estimated blue line) and nonlinear correlation observed between SPIE and precipitation. Interpreting predictions with the semi-variogram provides a better understanding of possible dependency dataset to each others and the generalized outputs. However, the model makes an enormous difference if the function is to be used for prediction (Fig. 2.7). For instance, as illustrated in Fig. 2.18a, the accumulation of NDVI values on the beginning of the curvature line shows positively, and more or less correlation is available between pairs 0.05, 0.20, and 1 between values. This is a nice example of the distinction between statistical significance and the scientific importance of the dataset. The curvature is highly significant and given a high variance in y, the effect of curvature is less effective, just a few distance (measured x) periods is effectively correlated. The curvature has to pass to the averaged dataset. In the case of the curvature model, no information on non-linearity other than that contained within data, then parsimony suggests that errors will be smaller using the simpler, linear model prediction (Fig. 2.17). We have applied a simple kriging standard error map (Fig. 2.6c) to receive fewer errors within applying certain datasets for the prediction status of patterns (loss and gain productivity) and resilience areas of Central Asia. Both models (Figs. 2.6 and 2.7) are equally good at describing the data ($r^2 = 0.76$) (the power law model) and $y = 0.96 * x + 0.80$, but extrapolation beyond the range of the data is always fraught with difficulties.

Explored relationships between temporal changes of SPIE events (1982–2015) and NDVI spatial patterns (1982–2015) for the arid and semi-arid zones of Central Asia (Fig. 2.6a, b) and linear relationships between varies: $y = 0.96 * x + 0.80$ (Figs. 2.6 and 2.7); also linear/positive relationship observed between periods of precipitation anomalies and high evapotranspiration ($Prec_{low}$ /$SPEI_{max}$), as observed regionally drought periods in Central Asia. The positive relationship means that SPIE is getting a peak period (plus ratings) and, the lowest ratings of precipitation is accumulated on same time.

Generally, drought ratings continues more than 90 days, prolongation droughts and more than 90 days associated with raising temperature ratings. In contrast, the main drought episodes were identified by the SPEI (Fig. 2.7) and NDVI values that illustrated vegetation accumulation ratings (0.02–0.43) (Fig. 2.7), when SPIE had evaporated under following indices: 0.06–0.41; The further anomalies scenarios regarding on datasets (Fig. 2.7), quantity of samples are equal to 1863 (as dots) and indicated linear regression when applied four certainty datasets (Prec/Temp/NDVI/SPIE). Moreover, if temperature increased progressively by 2° or 4 °C on the global level, the reinforcement of drought severity is associated with higher water demand

by potential evapotranspiration (Vicente-Serrano et al. 2015a, b). The similarity or progressive rise in temperature is already estimated in Turkmenistan, then in Uzbekistan and Kazakhstan.

2.3.5 *Ongoing Process and Early Drought Detection with the Kriging Method*

This research assessed the vegetation dynamics in Central Asian drylands to determine which associated anthropogenic pressures are versus climate anomalies. During high ET_0 is expected to continuous of decreasing levels of water resources, as shown in Fig. 2.17c, the rating of the negative vegetation values (Fig. 2.17) with high transpiration is forecast across the borders of Turkmenistan and Uzbekistan, Uzbekistan and Tajikistan, and Kyrgyzstan and small areas of Kazakhstan around the Kyzylkum Desert. The background of the prediction map (Fig. 2.17) illustrates improper low vegetation values in the southwestern part of the area (red color); it might be a landscape pattern these areas mostly under desert zones and vegetation patterns or coverage is frequently sparse.

Large-scale datasets are used to assess and measure relationships between global climate patterns and regional-scale vegetation responses to support land and water use and management in this drought-prone region with prediction map/trend. The prediction map (Fig. 2.18) illustrates a more complex situation for resiliency; among five countries only Kazakhstan and Kyrgyzstan are more resilient in this ongoing scenario, with projections suggesting losses in areas of Turkmenistan, Uzbekistan, Tajikistan, and partly Kyrgyzstan, and same time potential gains (increasing more greenness) in Kazakhstan lands. It is more important to see that a vast area of rangeland/grasslands are stabilizing or restoring in part of Kazakhstan. However, it is a vast country and on the regional or local level, we may find diverse problems related to anthropogenic effect or the climate change issue. A right example is that for Kyzylorda region; after rice paddying and high evapotranspiration in atmosphere, huge agricultural zones have been converted on saline and abandoned areas.

Some main affected areas among regions in Central Asia and mapping were identified with standard error for detection of change values or prediction standard errors (Fig. 2.17) quantify the uncertainty for each location in the surface that we created and developed criteria to illustrate vegetation loss areas. A simple rule of thumb is that 95% of the time, the true value of the surface will be within the interval formed by the predicted value. Appropriate phytoindicators for modifying and designing different ecological zones, especially trends of spatial changes of vegetation cover over time trends which are associated with climate patterns, assessed a better understanding vegetation movement dynamics and their mechanisms. Within prediction standard error surface that locations (five countries) near sample points generally have lower error and more accuracy for receiving further status of vegetation (Fig. 2.18).

On the basis of criteria to develop appropriate phytoindicators with fragile zones as lesser resilience of climate anomalies (regions of the country) are the following:

Turkmenistan: Balkan (I), Taschauz (II),

Uzbekistan: Ferghana (III), Namangan (IV), *Navoi* (V), Syrdaryo (VI), Karakalpakstan (VII), Khorezm(VIII)

Tajikistan: Khodjand (IX)

Kyrgyzstan: Batken (X), Naryn (XI),

Kazakhstan: Mangghystau (XII), Kyzylorda (XIII)

To resilience of this occasions or as a potential winner (Kazakhstan and partly Kyrgyzstan) and losers (Turkmenistan, Uzbekistan, and Tajikistan). This assumption will have to undertake proactive adaptation tools to reduce early drought damage for loser category countries. On the basis of results, we are able to forecast that two regions of Central Asia are detected as high potential risk zones: Turkmenistan and Tajikistan. Also, more than half the area of Uzbekistan is also indicated as same status.

2.4 Conclusion

The rising occurrence of drought events and following soil salinization are serious threats that have major impacts on land use and land cover (LULC) change patterns in agricultural zones of Central Asia. This research demonstrates that it is possible to estimate based on satellite image sources and effectively disseminate an early warning of disaster risk zones for upcoming months or years. For developing countries, there is increased awareness of the loss of biodiversity caused by abiotic stresses, especially drought events observed and characterized as a higher influence by agricultural sectors. Therefore, the drought is an occasional issue in Central Asia, and the minimum values have not reached the positive values, which means drought trends will be observed as longer or shorter term in all selected countries and regions. The strongest drought in past years was observed in Lebap (SPIE > -3) and in Naryn (SPIE > -3), also in GBAR region (SPIE > -2), while this region is famous with mountain ecosystems. Based on median values (Fig. 2.17, left side) in Central Asia drought or drought anomalies are observed usually in targeted areas (based on minus values). For selected areas, at least two times of peak drought periods were estimated, mostly in Turkmenistan, and after that in Uzbekistan. In general, arid and semi-arid regions particularly have high evaporation loss ratings, and therefore, high ET_0 ratings were observed, where the water supply is most limited and very valuable. Performance of utilization of satellite images within drought indexes gives affordable and visual information for current and past condition to analyze and develop information systems for early drought detection. Arid zones are prone to frequent seasonal droughts, and complex terrain that both hinders ground and satellite-based remote sensing is an applicability of conventional subgrid process to make parametrizations for detection of early drought anomalies with developing indicator approaches.

Acknowledgments The project work was financed by the DAAD Program, partly by GFF (TU-Dresden) through a research exchange between Central Asia and the European Union. We thank Prof. Elmar Csaplovics (TU-Dresden) for his potential interest for this area and supporting it. For the technical and statistical part we thank the colleagues of TU-Dresden, Institute Remote Sensing and Photogrammetry, for their expert assistance to simulate data with statistical approach and time series analysis.

References

Abdullaev I (2014) Water-energy-agriculture and environment nexus in Central Asia: current state and future. Presentation from the World Water Week, Stockholm, Sweden. http://programme.worldwaterweek.org/sites/default/files/water-energy food_and_environmental_nexus_in_central_asia.pdf

Abramowitz M, Stegun A (1965) Handbook of mathematical functions. Dover, New York

Aralova D, Toderich K, Jarihani B, Gafurov D Gismatulina L, Osunmadewa BA, Abualgasim R, Majdalin (2016) Environmental resilience of rangeland ecosystems: assessment drought indices and vegetation trends on arid and semi-arid zones of Central Asia. In: Proceedings of the SPIE 10005, earth resources and environmental remote sensing/GIS applications VII, 100050R (18 October 2016)

Bedunah DJ, McArthur ED, Fernandez-Gimenez M, eds (2006) Rangelands of Central Asia: proceedings of the conference on transformations, issues, and future challenges. 2004 January 27, Salt Lake City, UT. Proceedings RMRS-P-39. U.S. Department of Agriculture, Forest Service, Rocky Mountain Research Station, Fort Collins, 127 p

Beguería S, Vicente-Serrano SM, Reig F, Latorre B (2014) Standardized precipitation evapotranspiration index (SPEI) revisited: parameter fitting, evapotranspiration models, tools, datasets and drought monitoring. Int J Climatol 34(10):3001–3023. https://doi.org/10.1002/joc.3887

Bobojonov I, Aw-Hassan A (2014) Impacts of climate change on farm income security in central Asia: an integrated modeling approach. Agric Ecosyst Environ 188:245–255

Charusombat U, Niyogi D (2011) A hydroclimatological assessment of regional drought vulnerability: a case study of Indiana droughts. Earth Interact 15(26):1–65

Ciabatta L, et al (2016) Using Python® language for the validation of the Cci soil moisture products via Sm2Rain. 1–6. https://doi.org/10.7287/peerj.preprints.2131v1

FAOstat (2015) http://faostat3.fao.org/home/E. Accessed Mar 2015

Gasparrini A (2011) Distributed lag linear and non-linear models in R: The package dlnm. J Stat Softw 43:1–20

Gessner U, Naeimi V, Klein I, Kuenzer C, Klein D, Dech S (2012) The relationship between precipitation anomalies and satellite-derived vegetation activity in Central Asia. Glob Planetary Change 110:74–87. https://doi.org/10.1016/j.gloplacha.2012.09.007

Gintzburger G, Toderich K, Mardonov B, Mahmudov M (2003) Rangelands of the arid and semi-arid zones in Uzbekistan. CIRAD–ICARDA Montpellier, p 426

Gong Z et al (2017) Research on trend of warm-humid climate in Central Asia. IOP Conf Ser Earth Environ Sci 74:012017

Harris I, Jones PD, Osborn TJ, Lister DH (2014) Updated high-resolution grids of monthly climatic observations—the CRU TS3.10 Dataset. Int J Climatol 34(3):623–642

Jones PD, Harris IC (2008) Climatic Research Unit (CRU) time-series datasets of variations in climate with variations in other phenomena. NCAS British Atmospheric Data Centre, date of citation. http://catalogue.ceda.ac.uk/uuid/3f8944800cc48e1cbc29a5ee12d8542d

Kariyeva J (2011) Land surface phenological responces to land use and climate variation in a changing Central Asia. Dissertation. In: Johnson R (ed) Graduate College of University of Arizona, Tucson, p 179

Kariyeva J, van Leuwen WJD (2010) Environmental drivers of NDVI-based vegetation phenology in Central Asia. Remote Sens 3(2):203–246. https://doi.org/10.3390/rs3020203

Kerr YH et al (2012) The SMOS soil moisture retrieval algorithm. Geosci Remote Sens 50:1384–1403

Mirzabaev A, Guta D, Goedecke J, Gaur V, Börner J, Virchow D, Denich M, von Braun J (2015) Bioenergy, food security and poverty reduction: trade-offs and synergies along the water–energy–food security nexus. Water Int 40(5–6):772–790

Musyimi Z (2011) Temporal relationships between remotely sensed soil moisture and NDVI over Africa: potential for drought early warning? pp 1–49

Nicholson SE, Tucker CJ, Ba MB (1998) Desertification, drought, and surface 1055 vegetation: an example from the West African Sahel. Bull Am Meteorol Soc 79:815–829

Paulik C, et al (2014) Open source toolbox and web application for soil moisture validation. In: IEEE geoscience and remote sensing symposium, pp 3331–3333. https://doi.org/10.1109/IGARSS.2014.6947193

Peel MC, Finlayson BL, McMahon TA (2007) Updated world map of the Köppen-Geiger climate classification. Hydrol Earth Syst Sci 11(5):1633–1644

Pickup G (1998) Desertification and climate change—the Australian perspective. Clim Res 11:51–63

Propastin PA, Kappas M, Muratova NR (2008) A remote sensing based monitoring system for discrimination between climate and human-induced vegetation change in Central Asia. Manag Environ Qual Int J 19(5):579–596. https://doi.org/10.1108/14777830810894256

Squires V (2012) Rangeland stewardship in Central Asia: balancing improved livelihoods, biodiversity conservation and land protection. ISBN 978-94-007-5366-2. https://pasture.klink.asia/klink/9c1102/download?embed=true

Ta Z, Yu R, Chen X, Mu G, Guo Y (2018) Analysis of the spatio-temporal patterns of dry and wet conditions in Central Asia. Atmosphere 9(1). https://doi.org/10.3390/atmos9010007

Thenkabail PS, Knox JW, Ozdogan M, Gumma MK, Congalton RG, Wu Z, Milesi C, Finkral A, Marshall M, Mariotto I, You S, Giri C, Nagler P (2012) Assessing future risks to agricultural productivity, water resources and food security: how can remote sensing help? Photogramm Eng Rem S 78(8):773–782

Toderich K, Shuyskaya E, Taha FK, Matsuo N, Ismail S, Aralova D, Radjabov T (2013) Integrating agroforestry and pastures for soil salinity management in dryland ecosystems in Aral Sea basin. In: Developments in soil salinity assessment and reclamation, pp 579–602

Touge Y, Tanaka K, Khujanazarov T, Toderich K, Kozan O, Nakakita E (2015) Developing a water circulation model in the Aral Sea Basin based on in situ measurements on irrigated farms. J Arid Land Stud 25(3):133–136

Tucker CJ, Pinzon JE (2013) A 1981–2012 non-stationary AVHRR NDVI global 8-km data set AGU fall meeting abstracts

Udelhoven T, Stellmes M, del Barrio G, Hill J (2009) Assessment of rainfall and NDVI anomalies in Spain (1989–1999) using distributed lag models. Int J Remote Sens 30:1961–1976

Vicente-Serrano SM, Begueria S, Lopez-Moreno JI, Angulo M, El Kenawy A (2010) A new global 0.5 degrees gridded dataset (1901–2006) of a multiscalar drought index: Comparison with current drought index datasets based on the Palmer Drought Severity Index. J Hydrometeorol 11:1033–1043. https://doi.org/10.1175/2010JHM1224.1

Vicente-Serrano SM et al (2015a) Drought variability and land degradation in semiarid regions: assessment using remote sensing data and drought indices (1982–2011). Remote Sens 7:4391–4423

Vicente-Serrano SM, Cabello D, Tomas-Burguera M, Martin-Hernandez N, Beguera S, Azorin-Molina C, Kenawy AE (2015b) Drought variability and land degradation in semiarid regions: assessment using remote sensing data and drought indices (1982–2011). Remote Sens 7(4):4391–4423. https://doi.org/10.3390/rs70404391

Vicente-Serrano SM, Tomas-Burguera M, Beguería S, Reig F, Latorre B, Peña-Gallardo M, Luna MY, Morata A, González-Hidalgo JC (2017) A high resolution dataset of drought indices for Spain. Data 2:22

Wardlow B, Anderson M, Verdin J (eds) (2012a) Remote sensing of drought. CRC Press, Boca Raton

Wardlow BD, Anderson MC, Sheffield, J, Doorn, BD, Verdin, JP, Zhan X, Rodell M, Future Opportunities and Challenges in Remote Sensing of Drought (2012b) Drought Mitigation Center Faculty Publications. p 103. http://digitalcommons.unl.edu/droughtfacpub/103